CHAPTER 3

Methodology

3.1 Workflow

The workflow of this study consists of 3 main steps that are 1) Rock physics and AVO modeling, 2) Pre-stack deterministic inversion, and 3) Lithology delineation and prospect identification. The detail of each step will present as follows.

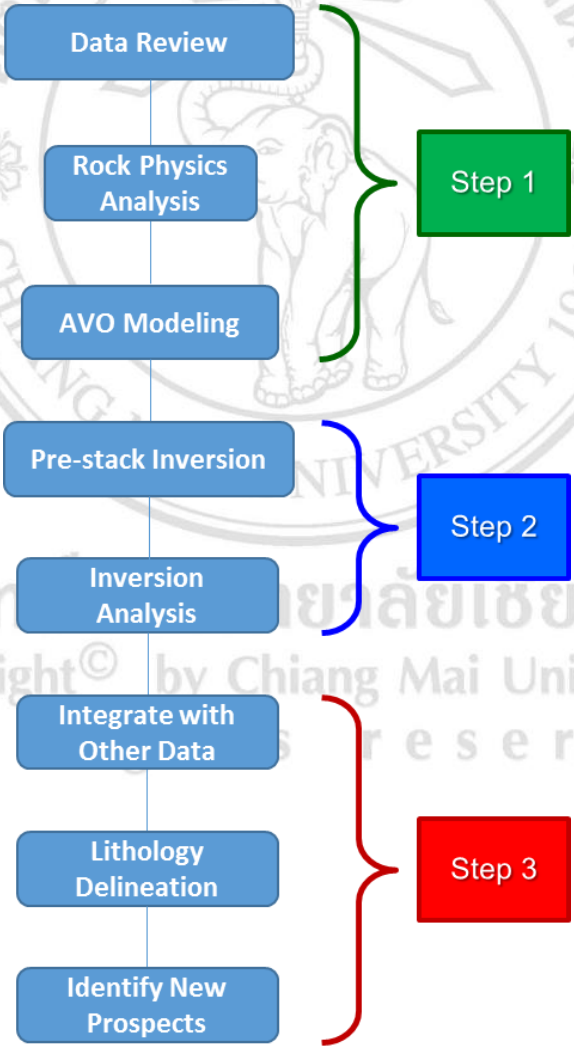

Figure 3-1. Simplified workflow of methodology

3.2 Rock Physic and AVO Modeling

3.2.1 Well Log Conditioning

Before conducting rock physics and AVO analysis, well log conditioning and quality control should be done using Petrel software because quality of the well log data sets especially sonic log (both compressional and shear sonic logs) are being affected by borehole conditions and changing borehole sizes. To ensure the high quality of the input well logs for pre-stack inversion and consequent results, bad data points were removed. Firstly, the well logs should be edited by deleting bad zone such as casing interval. Then, de-spiking of sonic logs was performed to eliminate the anomaly values. Next, the sonic logs were calibrated with checkshot or VSP data for correcting time-depth relationship and velocity. Finally, sonic log of each well conditioning step was compared to observe changing.

1) Well Log Edition. To improve well log quality, it is crucial to adjust or eliminate sections of well logs which are affected by poor borehole condition such as change of borehole sizes and a part of casing. Moreover, the poor sections of the well logs that are consequences from other methods of log editing or future processes should be also removed after finishing each process. For example, the P-wave sonic logs which were removed poor intervals are shown in Panel B of Figures 3-2 to 3-5.

2) Well Log De-spiking. The spikes from the log should be removed base on the selected filter and the distribution of the data at the locations within the filter. A filter width is defined and then the mean and standard deviation of the points within the filter are calculated. The log value which falls outside the standard deviation will be removed. The de-spiked P-wave sonic logs are shown in Panel C of Figures 3-2 to 3-5. Because of good well log data, the spikes of each well are small and difficult to observe.

3) Sonic Log Calibration. The purpose is correlation between checkshot and sonic travel times in wells by adjusting time of integrated sonic log to match smoothed checkshot times. The calibration is done by slightly increasing or decreasing the sonic values between checkshot points until the travel times of sonic log are corrected to the derived times from the checkshot survey. The calibrated sonic logs are represented in Panel D (red curves) and Panel G (blue curves) of Figures 3-2 to 3-5.

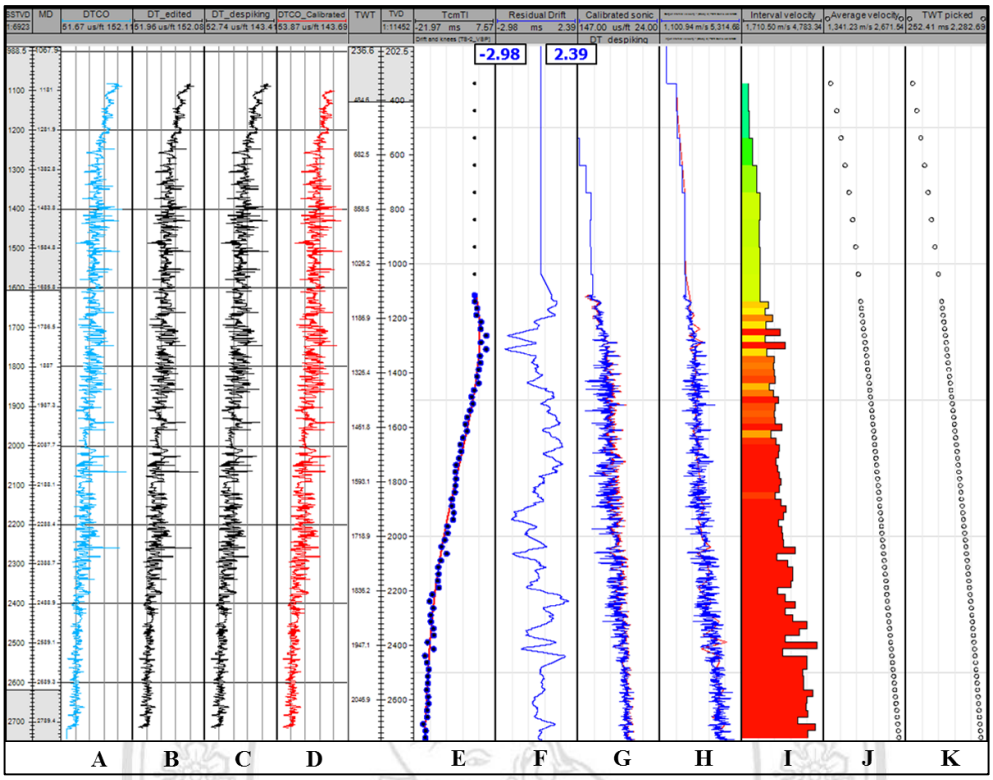

Figure 3-2. Sonic log conditioning of S-2 Well after calibration with checkshot using polynomial fit order 4 of created knees

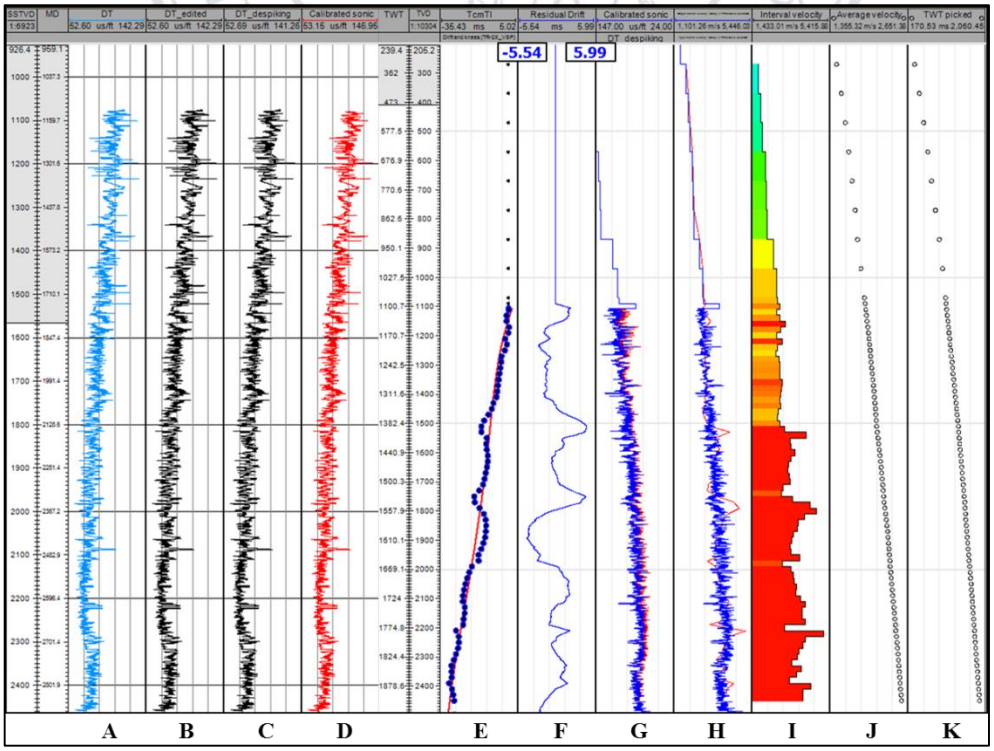

Figure 3-3. Sonic log conditioning of R-2 Well after calibration with checkshot using polynomial fit order 4 of created knees

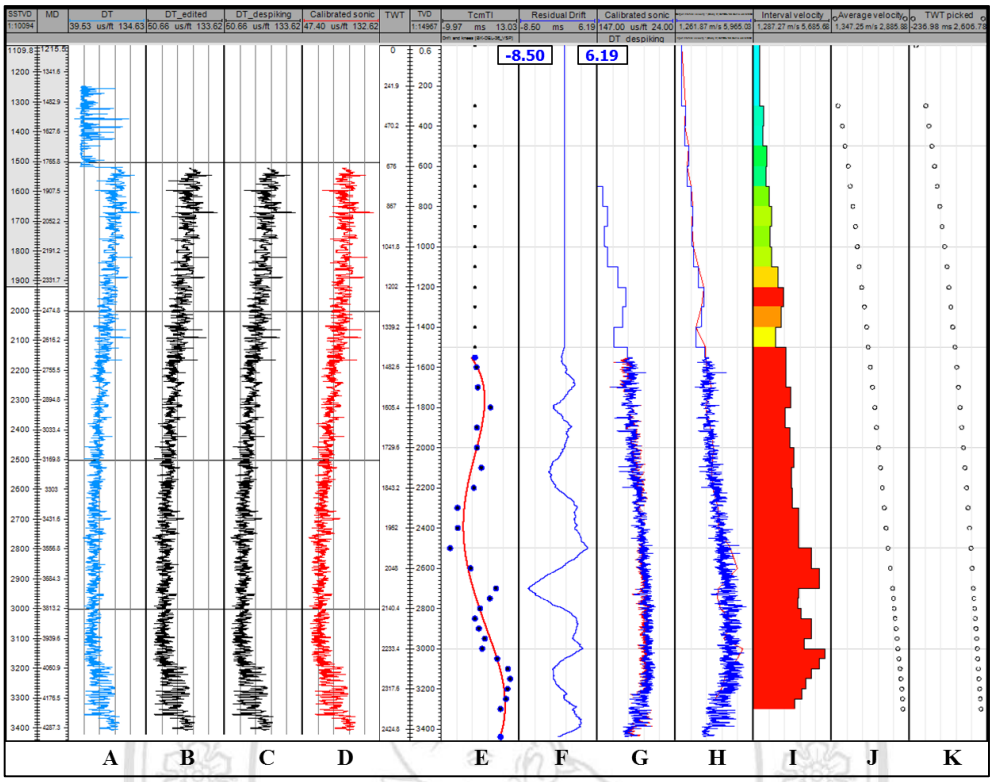

Figure 3-4. Sonic log conditioning of D-36 Well after calibration with checkshot using polynomial fit order 3 of created knees

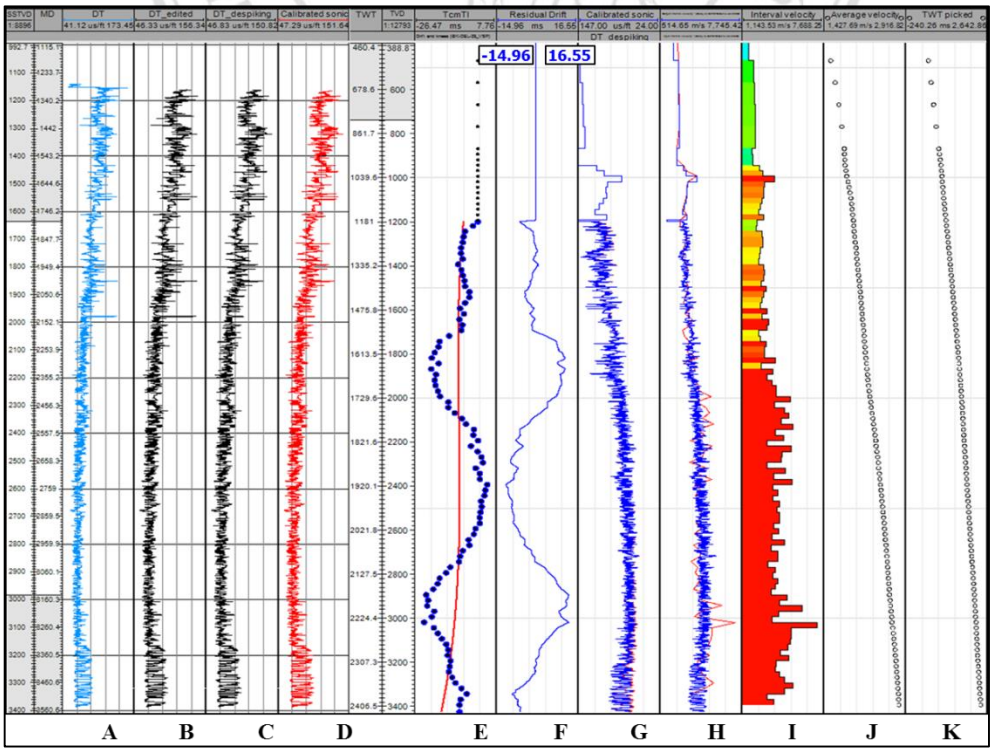

Figure 3-5. Sonic log conditioning of G-29 Well after calibration with checkshot using polynomial fit order 3 of created knees

Notes; alphabets in Figures 3-2 to 3-5 are referred to **Panel A:** initial log, **Panel B:** edited log, **Panel C:** de-spiked log, **Panel D:** calibrated log, **Panel E:** polynomial fit to VSP, **Panel F:** residual drift, **Panel G:** comparison of before (blue) and after (red) calibrated sonic logs, **Panel H:** converted V_P log (blue) and calculated interval velocity (red), **Panel I:** interval velocity, **Panel J:** average velocity and **Panel K:** two way time.

3.2.2 Shear Wave Velocity Estimation

In this study, small length of shear sonic log is available (Figure 1-7) then V_S estimation from V_P for the other regions is unavoidable. The general empirical relation for V_S estimation from V_P in brine-saturated rock is given by Castagna et al (1985), and Greenberg and Castagna (1992).

In D-36 well, the V_S is estimated using V_P and V_S crossplot from available data of lower section in FM1 (yellow highlight). It is important to divide available log to different interesting zones to each units for analyzing data and getting constants within the zone. The empirical relation equations of sandstone and shale which are published by Greenberg and Castagna (1992) are shown in yellow and green line, respectively (Figure 3-6). However, these lines were observed poor matching with data of this area, so new fit lines are calculated for sand (purple line) and shale (red line) (Figure 3-6).

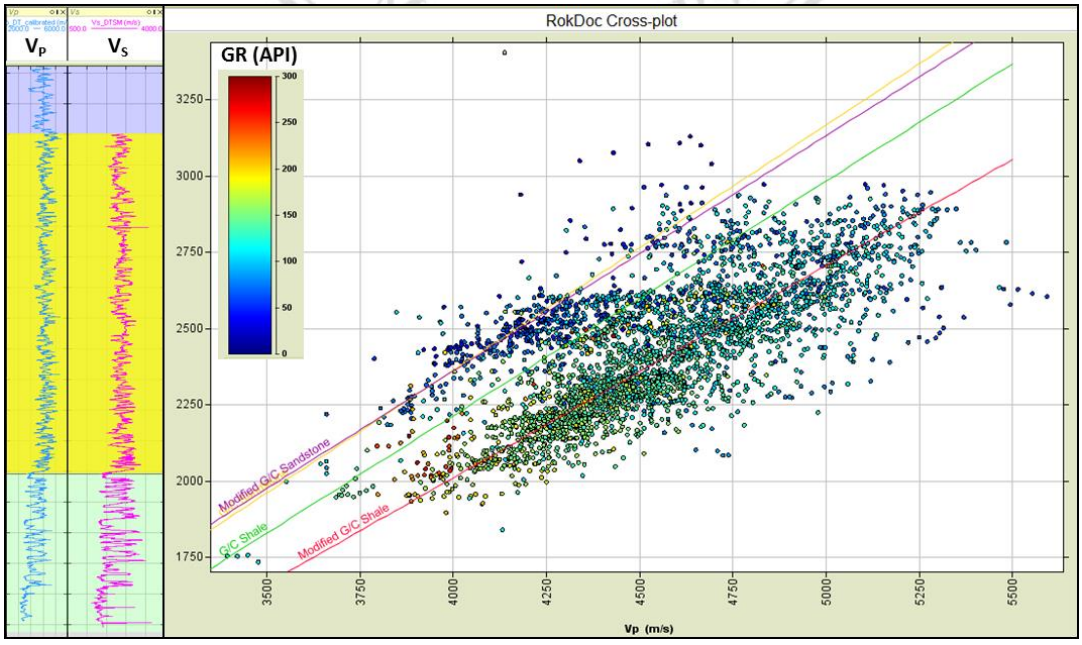

Figure 3-6. The highlight zone of V_P and V_S (yellow) that was used in V_P -V_S crossplot to find the best fit lines of sand and shale for estimating V_S in D-36 well.

The equations for V_S prediction were defined as:

Sandstone: $V_S = 0.7717V_P - 727.2$ (m/s) (3.1)

Shale: $V_S = 0.6959V_P - 775.3$ (m/s) (3.2)

The shear wave velocity logs were estimated from V_P using equations 3.1 and 3.2 for V_S of sand and V_S of shale, respectively. However, each log did not completely match with the original V_S log, because the original V_S log was acquired from formation which is normally comprised of both sand and shale layers. Therefore, to combine these two logs relating to lithology, Log Calculator of RokDoc software was used by defining if-cause equation which sand layers use V_S of sand and other use V_S of shale. Finally, the estimated V_S log (or combined V_S log) is used for the upper section where does not have V_S data, and the lower section have still used the original V_S log (Figure 3-7)

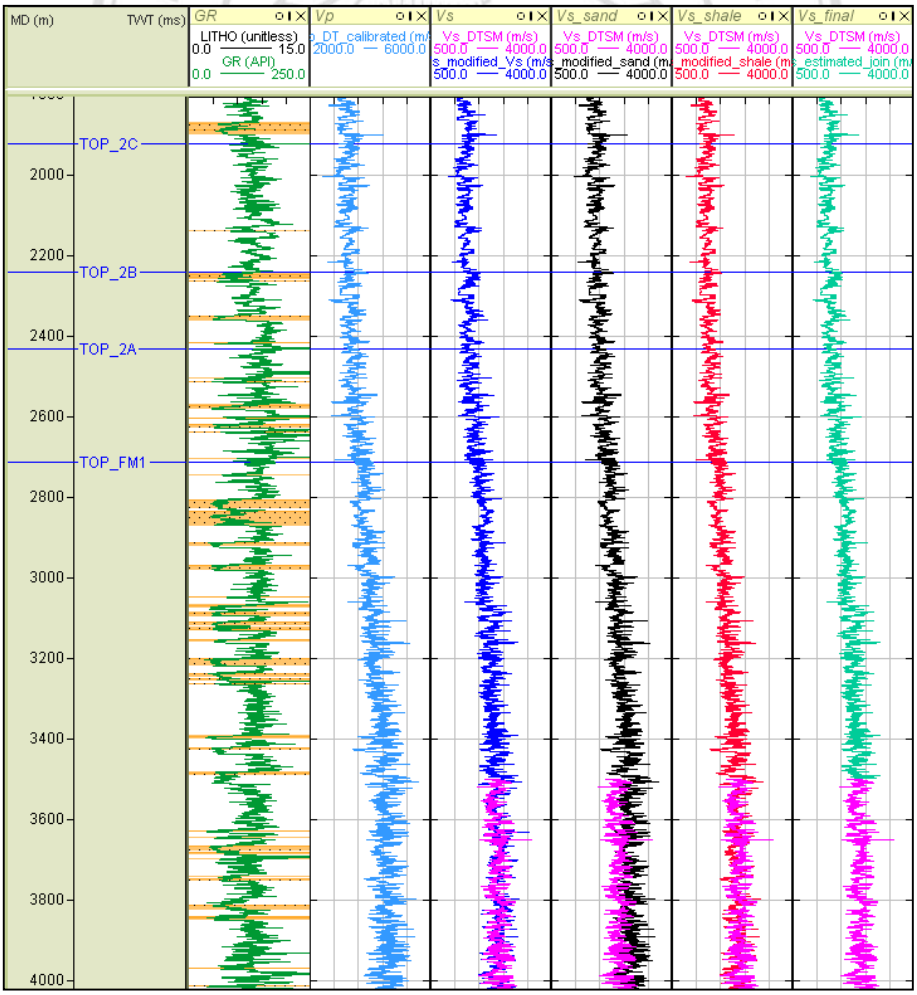

Figure 3-7. Log curves in V_S estimation are GR (green), V_P (light blue), original V_S (pink), combined V_S (blue), V_S sand (black), V_S shale (red), and final V_S (light green).

3.2.3 Rock Physics Model

Rock physics models are used to analyze the relationship of each elastic property such as V_P versus V_S and V_P versus density to achieve the understanding of rock properties which is directly related to seismic reflection responses. Well log data is important data to use in rock physics model. Crossplots of them are used to discriminate the lithology and fluid content of each rock units. Some of the rock physics models are used in this study showing below.

1. P-wave velocity and density relations (Gardner's relation) are used to define trends of rock types. In this study, the crossplot of P-wave velocity (V_P) and density for all well is represented shale trend and sandstone trend along with Gardner's shale line (green line) and sandstone line (orange line) (Figure 3-8). However, crossplots of each well are shown that the most of shale data (green to red of gamma ray color bar) is above Gardner's shale line (Figures 3-9 to 3-12). For sandstone (dark blue to cyan of gamma ray color bar) of each well, the most of data is corresponded to Gardner's sandstone line except S-2 well which shows quite low density at shallow part (red circle in Figure 3-9). From well report, the low density data is in unconsolidated interval, so they are low density and velocity.

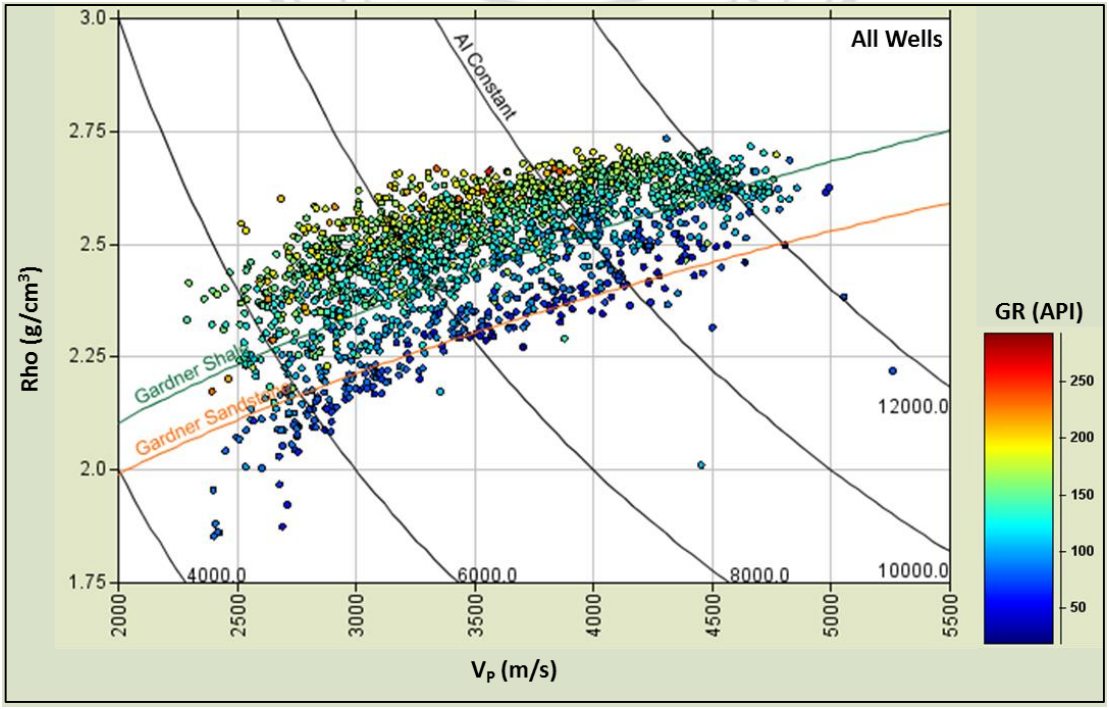

Figure 3-8. V_P-Rho crossplot of four wells (S-2, R-2, D-36 and G-29)

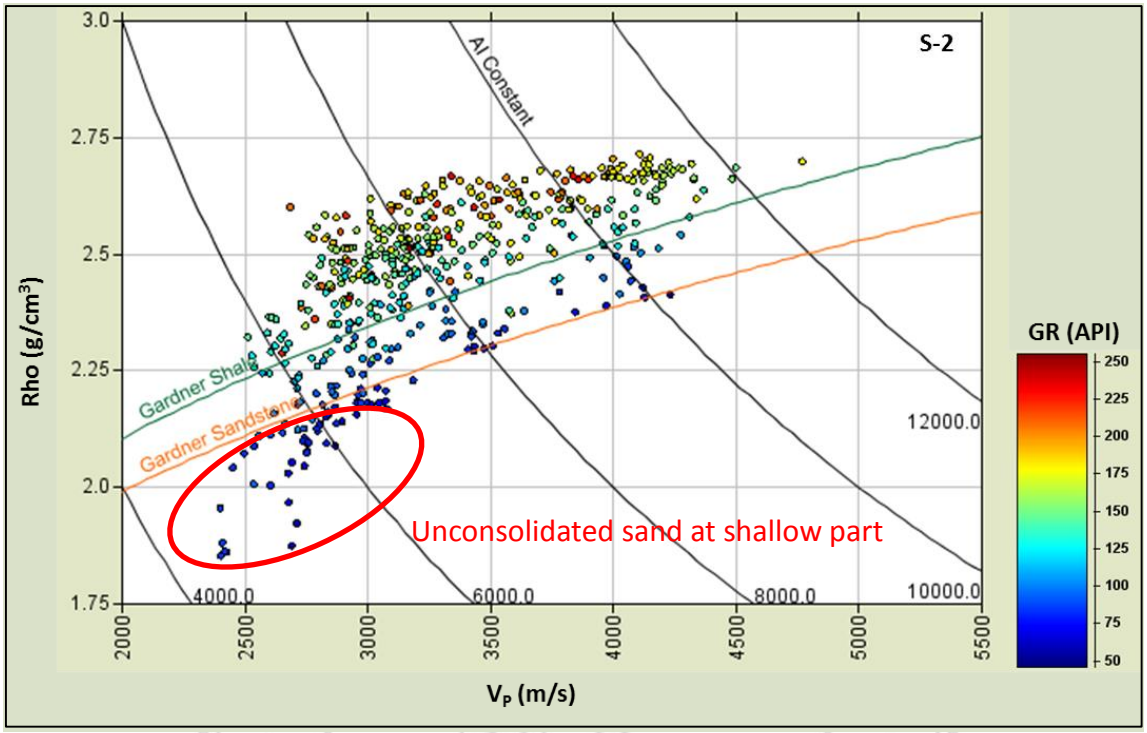

Figure 3-9. V_P-Rho crossplot of S-2 well

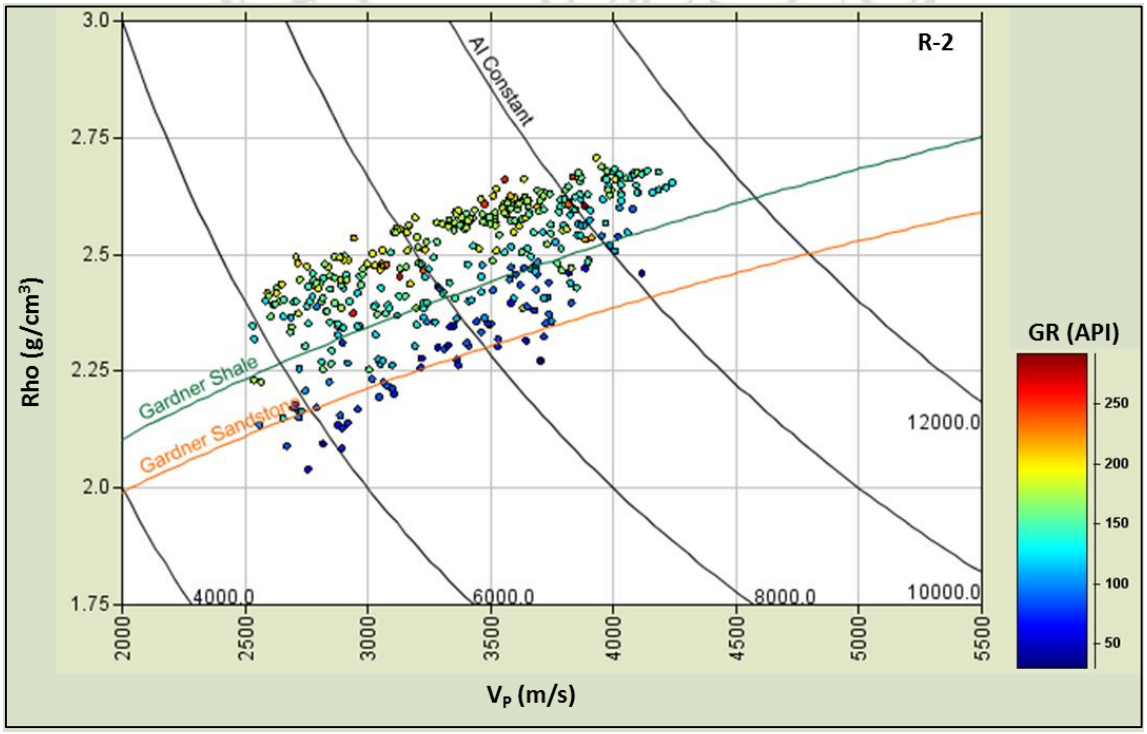

Figure 3-10. V_P-Rho crossplot of R-2 well

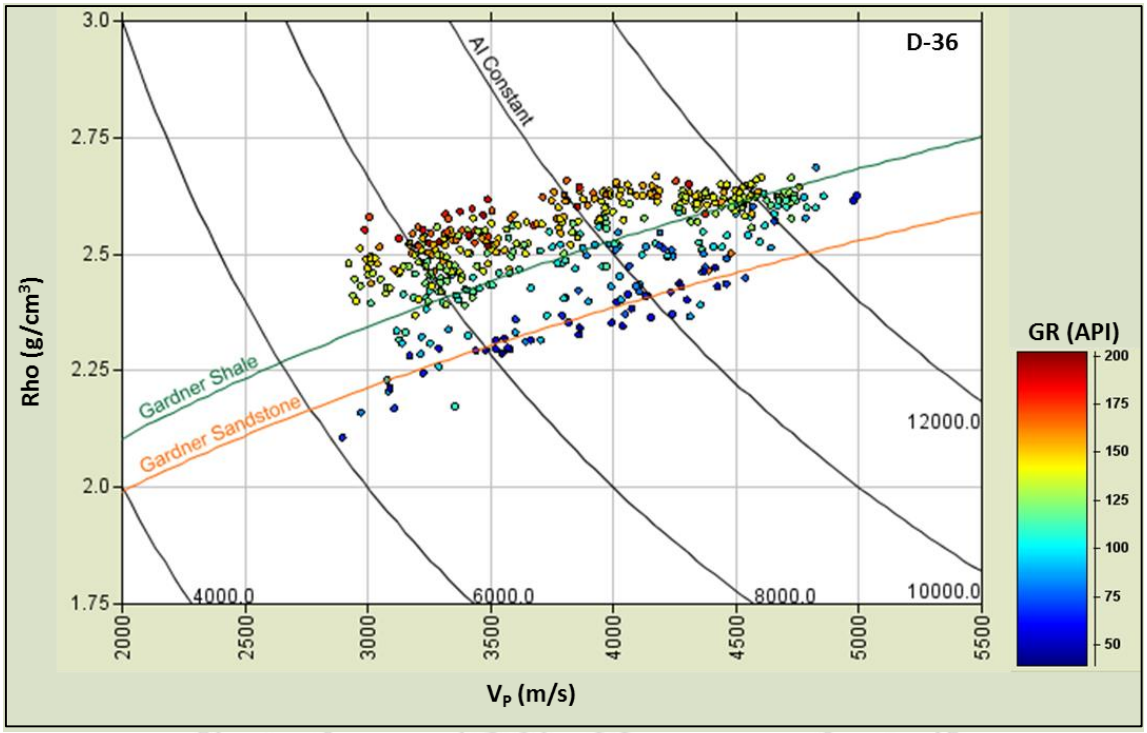

Figure 3-11. V_P-Rho crossplot of D-36 well

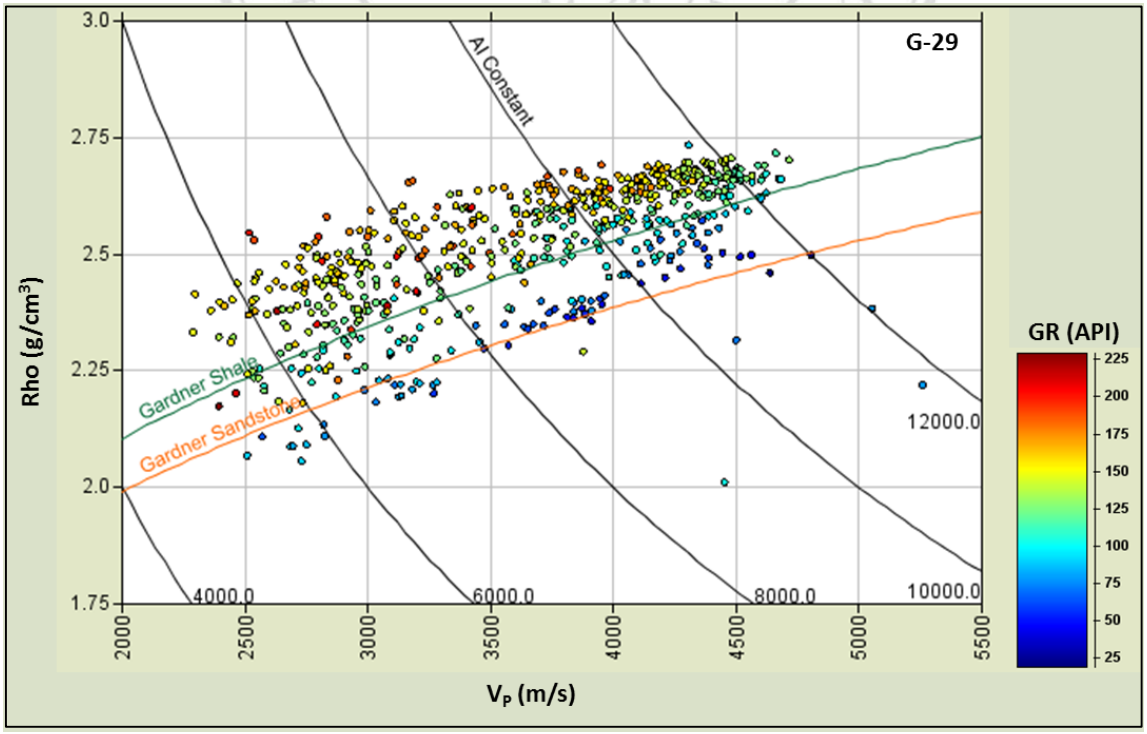

Figure 3-12. V_P-Rho crossplot of G-29 well

2. P-wave and S-wave velocity relations (Greenberg-Castagna relation) can be used to differentiate the lithology and it can be also providing V_P/V_S constraints in elastic inversion and log analysis. From V_P-V_S crossplots of each well in this area, they were clearly shown lithology trends (sandstone trend in blue circle and shale trend in red circle). However, at the same well, each interval of formation and unit was represented different trends at positions of sandstone and shale (Figures 3-13 to 3-15).

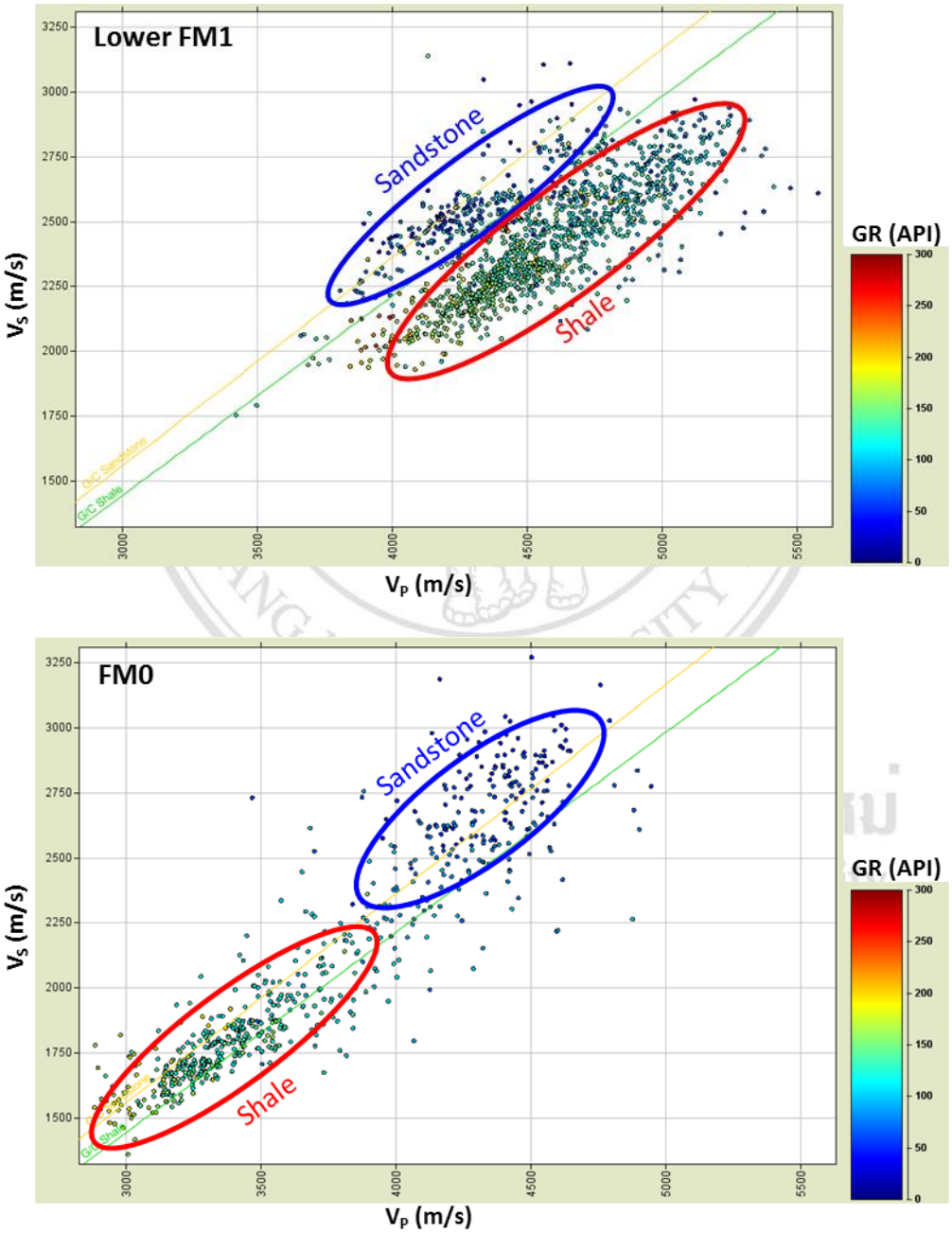

Figure 3-13. V_P-V_S crossplot of D-36 well at Lower FM1 and FM0 where were acquired S-wave velocity are shown different shale and sandstone trends.

To observe the available data in the V_P-V_S crossplots of each well, V_P and V_S values of deep section (FM1 and FM0) are faster than shallow sections (Unit 2D to 2A) because of high compaction increase with depth. However, FM0 in D-36 well, both V_P and V_S of the shale in this interval is quite low comparing to sandstone in the same section and shale in another formation (Figure 3-13). From well report, pressure profile show abnormal pressure in this formation, so it might be affected to velocity of shale.

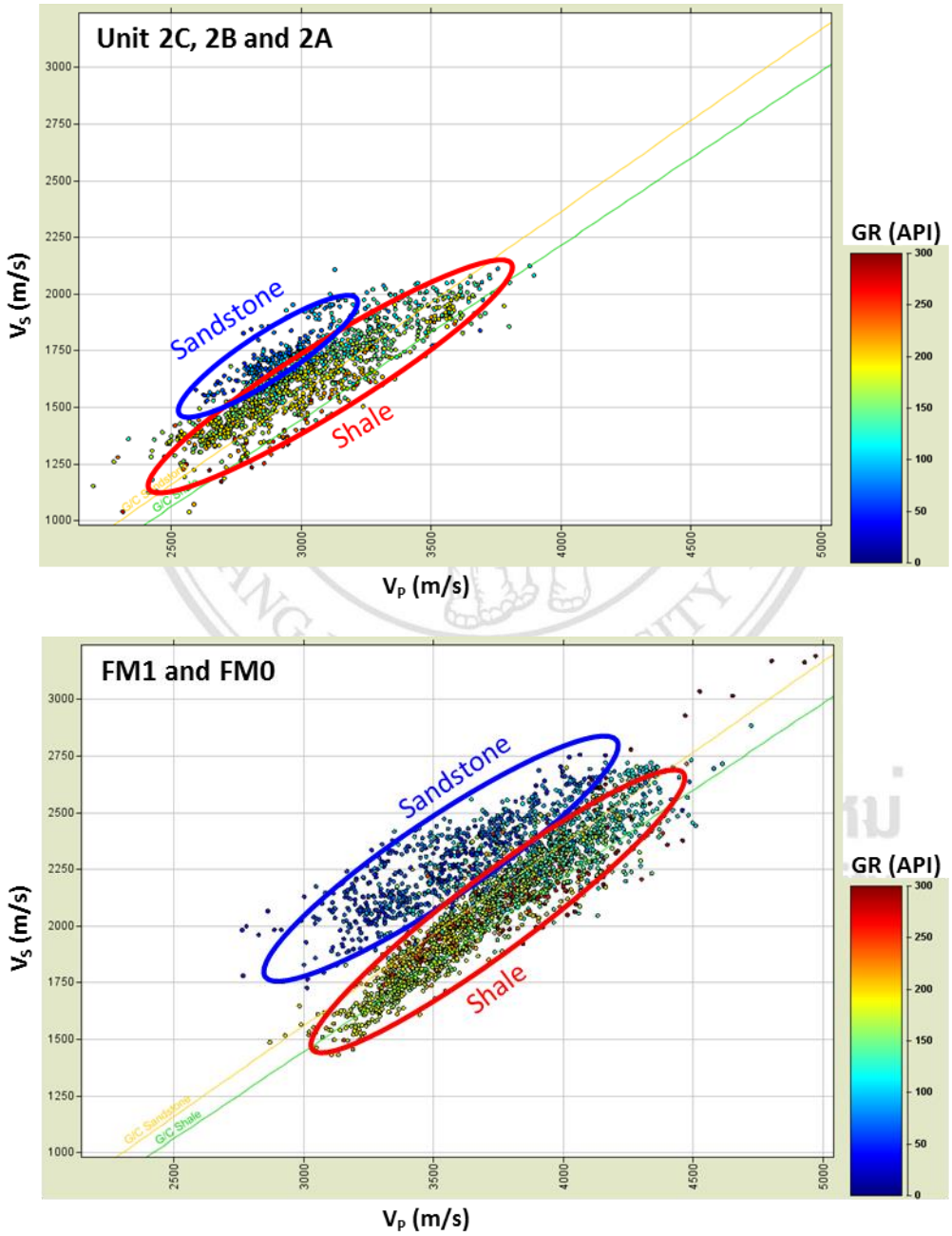

Figure 3-14. V_P-V_S crossplot of R-2 well at Unit 2C to 2A (above) and FM1 to FM0 (below) showing different shale and sandstone trends

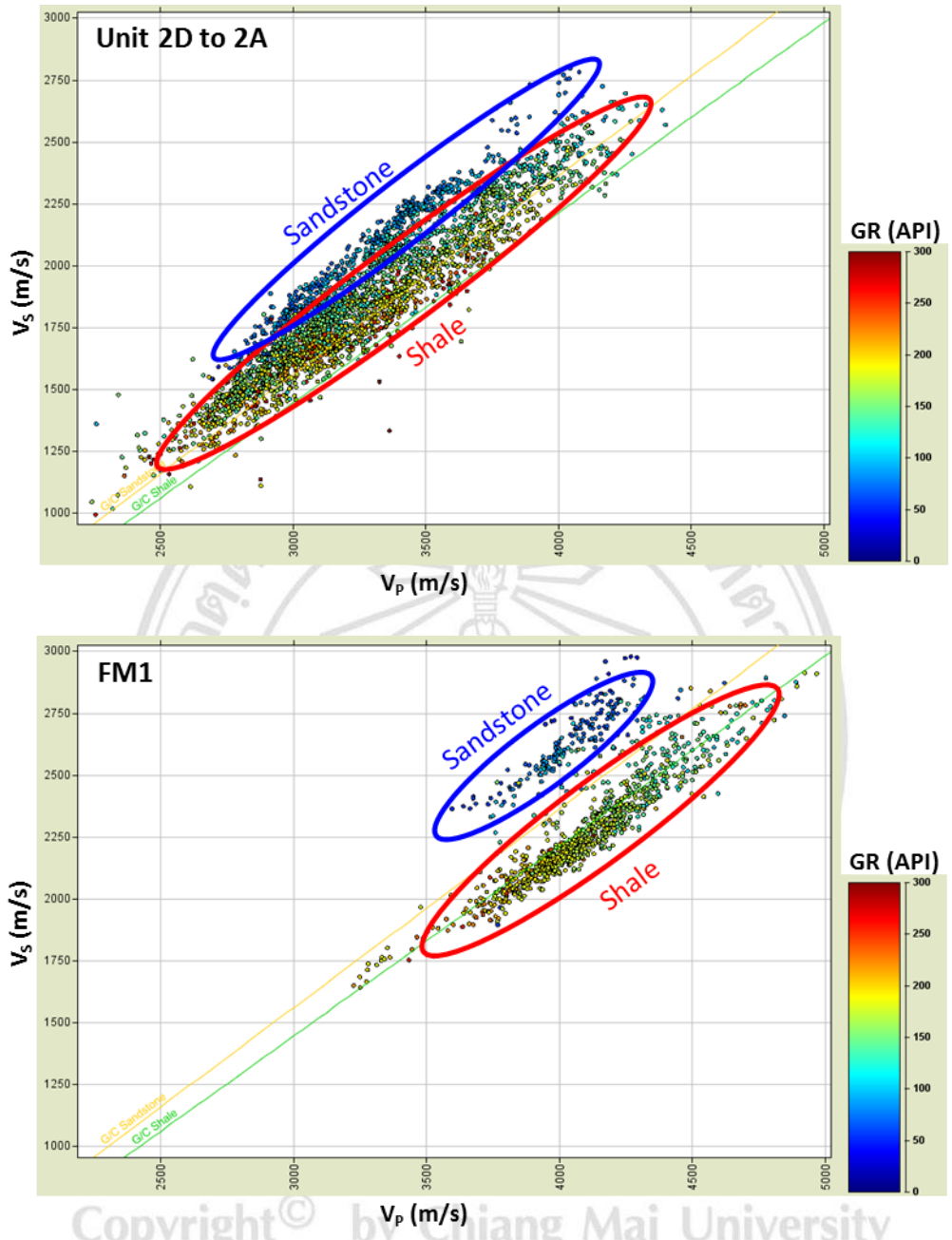

Figure 3-15. V_P-V_S crossplot of S-2 well at Unit 2D to 2A (above) and FM1 to TD (below) showing different shale and sandstone trends

Indeed, the crossplots between P-wave and S-wave velocity of the study can identify the lithology into sandstone and shale trends comparing to Greenberg-Castagna lithology lines in each working interval (formation and units). However, it is difficult to identify the saturated fluid in sandstones because low porosity values and high compacted rocks in the reservoir section are shown in well reports.

3.2.4 AVO Modeling

AVO modeling uses blocky models to analyze the AVO classes and responses based on well log data. The AVO modeling was carried out for each well using AVO classification which was plotted by the reflection coefficient (RC) and incidence angle (AVO plot). The plots show the responded curves of the top and base sandstone from near to far angle (0 to 40 degree) that mean the curves relating to interface of difference rocks. The interface reflectivity was calculated using 2 terms of Aki and Richards' approximation of the Zoeppritz equations (Aki and Richards, 1980) by plotting incidence angle (θ) on horizontal axis and RC on vertical axis. Then, the AVO classes can be considered to Class I, II, IIp, III and IV as shown in Table 2.1.

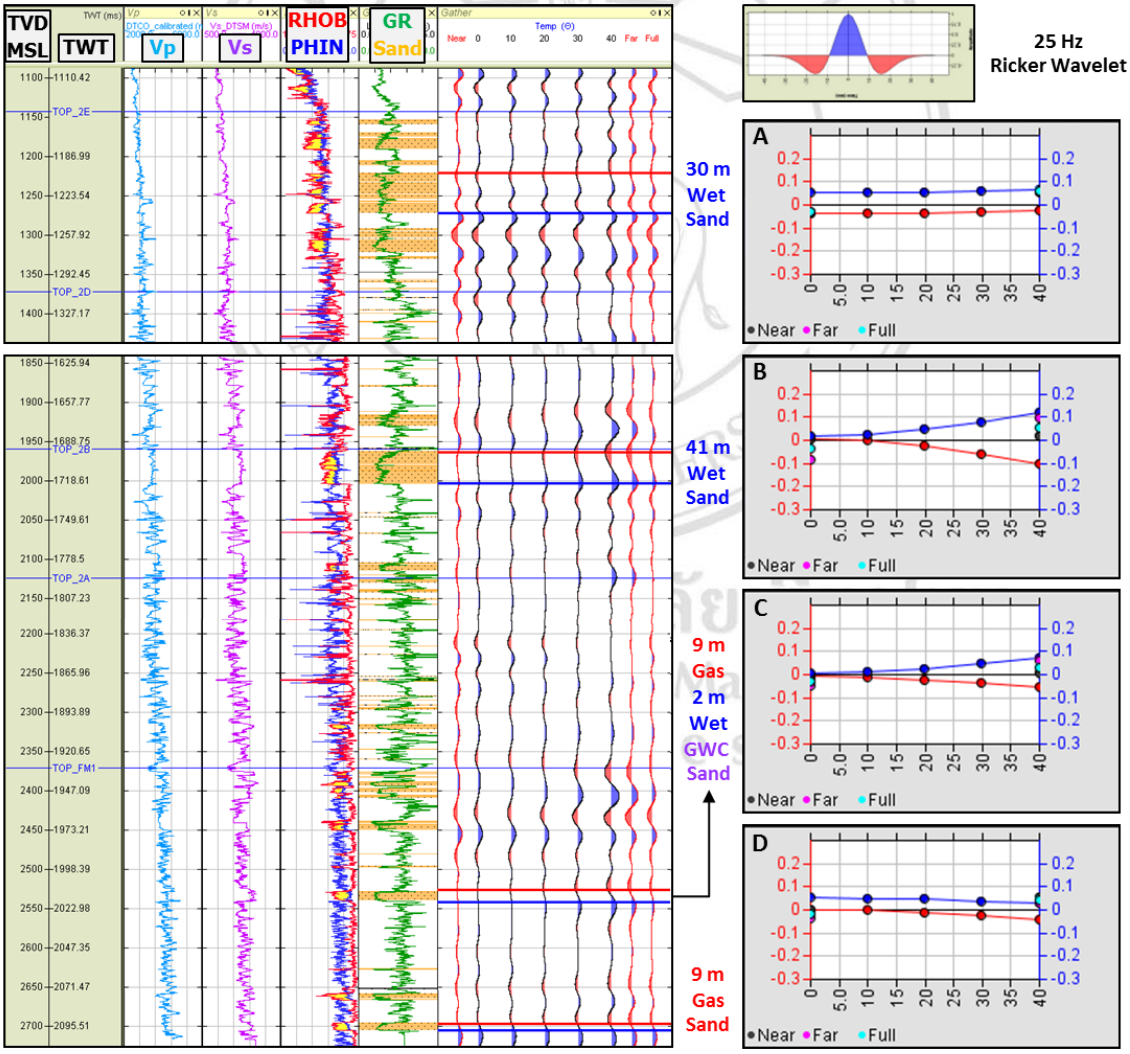

Figure 3-16. AVO modeling of S-2 Well shows example of water and gas sandstones. Sandstone A shows AVO class IV, sandstone B, C and D show AVO class II.

The AVO modeling is generated using well log data (V_P, V_S and density) and 25 Hz of Ricker's wavelet. For examples AVO models of saturated sandstones in each well, they represented different classes in wet (water) and gas sandstones. In S-2 well (Figure 3-16), curve (red) of top wet sandstone A which is in Unit 2E shows AVO class IV slightly increasing RC with increased angle. In contrast of wet sandstone B in Unit 2B, it shows class II that RC is near zero at the near angle and decreases with increased angle. This is abnormal for wet sandstone of this study area because it similar to gas sandstone C and D in Formation1 (FM1) which also show AVO class II. Normally, most of wet sandstones in this well and other wells are usually represented AVO class IV, and gas sandstones are often shown class II.

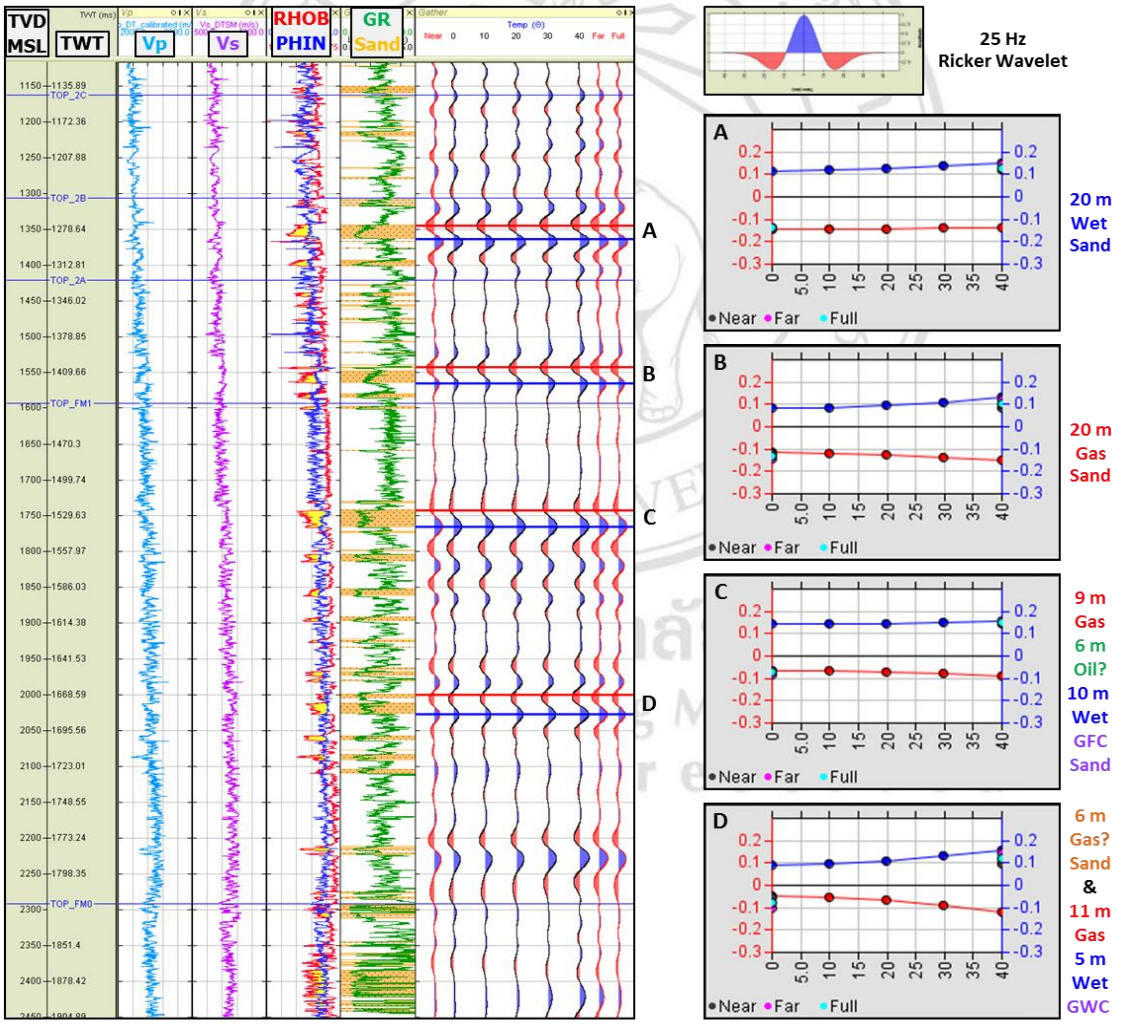

Figure 3-17. AVO modeling of R-2 Well shows example of water and gas sandstones. Sandstone A shows AVO class IV, sandstone B, C and D show AVO class II.

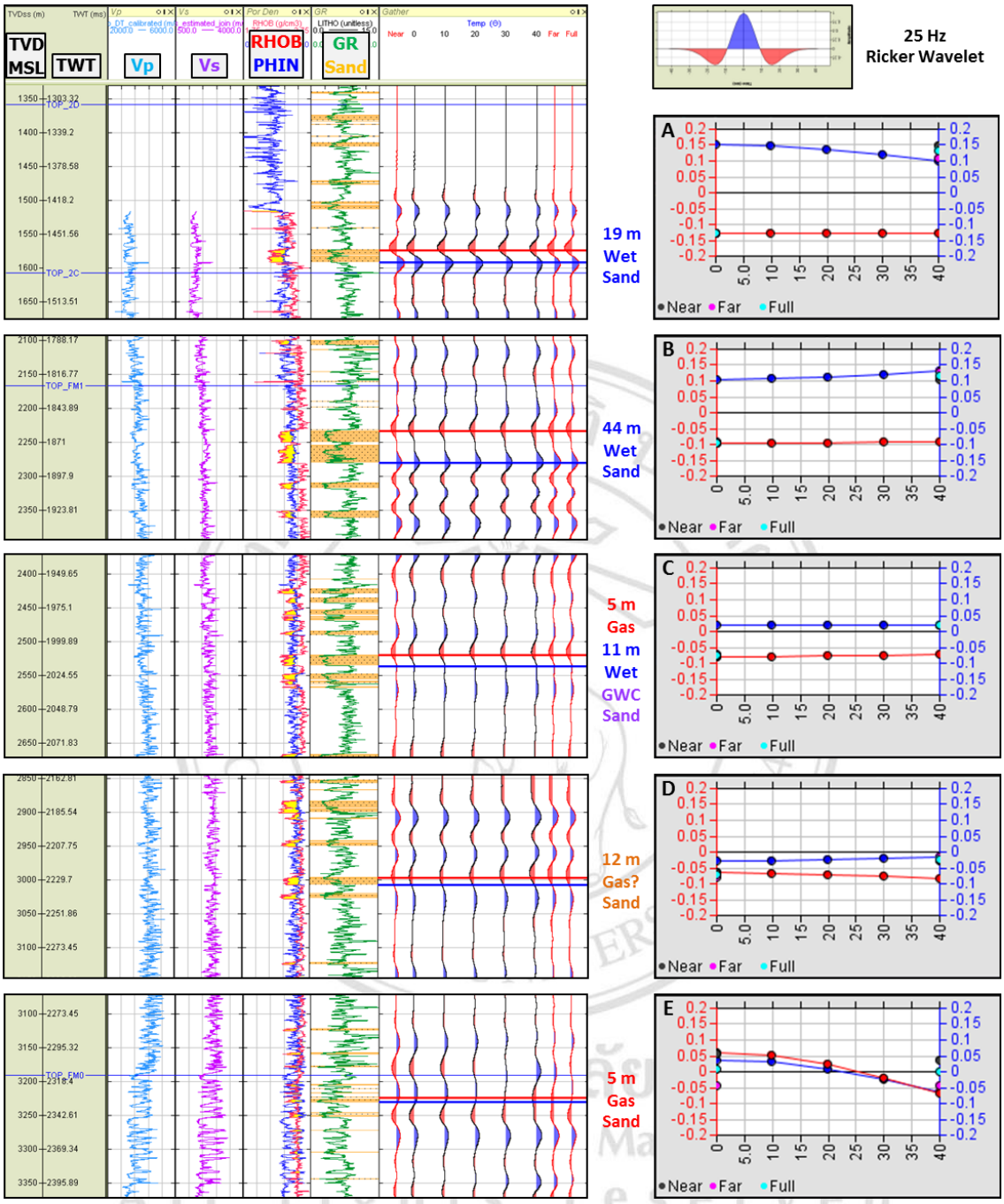

Figure 3-18. AVO modeling of D-36 Well shows example of water and gas sandstones. Sandstone A, B and C show AVO class IV, sandstone D shows AVO class II, sandstone E shows AVO class IIp.

In R-2 well (Figure 3-17), AVO synthetic gather at top of wet sandstone A is represented AVO class IV which RC slightly increases, but gas-bearing sandstone B shows AVO class II which RC slightly decreases with increasing angle. For sandstone C and D, they are filled with more than one type of fluid but are also displayed AVO

class II because they are affected with gas in the top of sandstone. D-36 (Figure 3-18) which is quite deep was divided into different intervals. Wet sandstone A in Unit 2D and wet sandstone B in upper FM1 of this well are shown quite constant curve of RC on top of rocks, so they should be the AVO class IV. Sandstone C which is filled with both gas and water is also represented AVO class IV because the model may be affected with the thicker layer of water. Sandstone D that is reported as possible gas because of quite low gas saturation is represented AVO class III similar to other gas sandstones in other wells. In Formation 0 (FM0), the thin gas sandstone E is represented AVO class IIp that displays positive RC at near angle and changes phase to negative at far angle. In conclusion of AVO plots, they can be represented in crossplots between intercept and gradient in Figure 3-19.

To be concerned that the reservoirs in this study area are quite thin and stacked layer sandstones, seismic resolution of synthetic traces and AVO responses to them should be take into account.

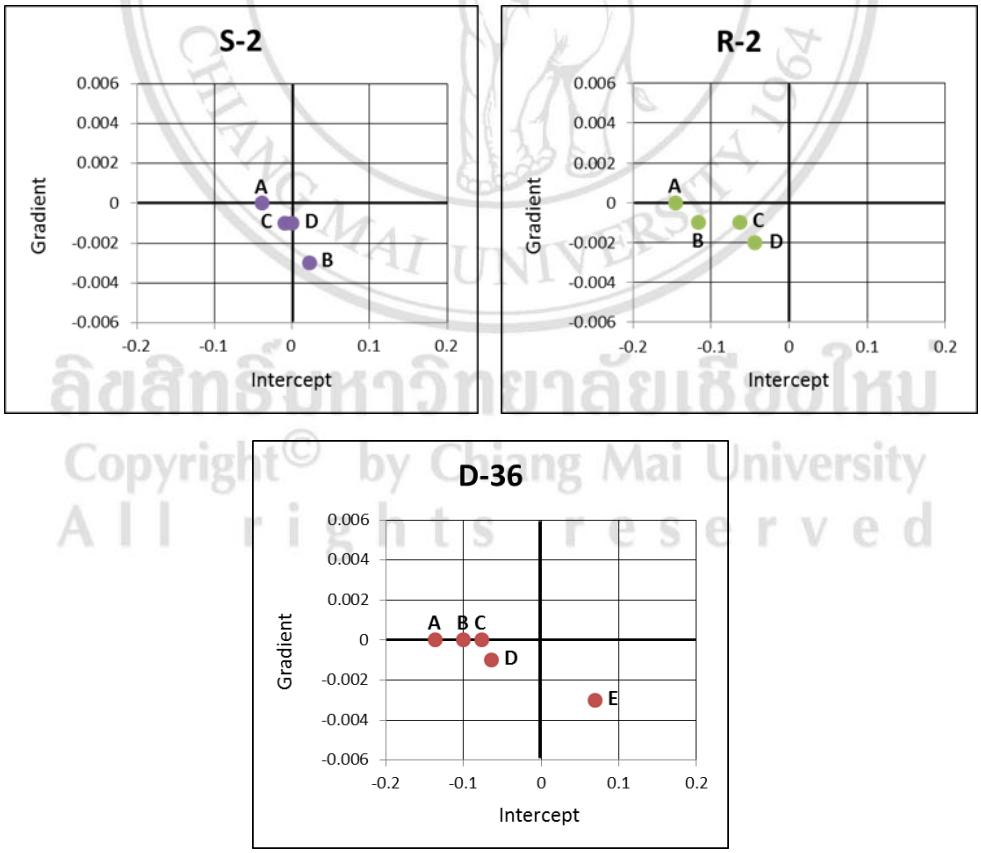

Figure 3-19. AVO crossplots between intercept and gradient of sandstones in S-2, R-2 and D-36 wells

3.3 Pre-stack Deterministic Inversion

Pre-stack inversion in this study is referred to simultaneous inversion because of dealing with different angle gathers parallel and deriving P-wave impedance (Z_P) and S-wave impedance (Z_S) together with density. It is better to perform of fully-processed pre-stack data in the angle domain to create Z_P, Z_S and density volumes. Pre-stack inversions are more useful for analysing the lithology and fluid contents of potential reservoirs than post-stack inversion. The workflow of pre-stack inversion in Hampson-Russell Suite software is illustrated in Figure 3-20.

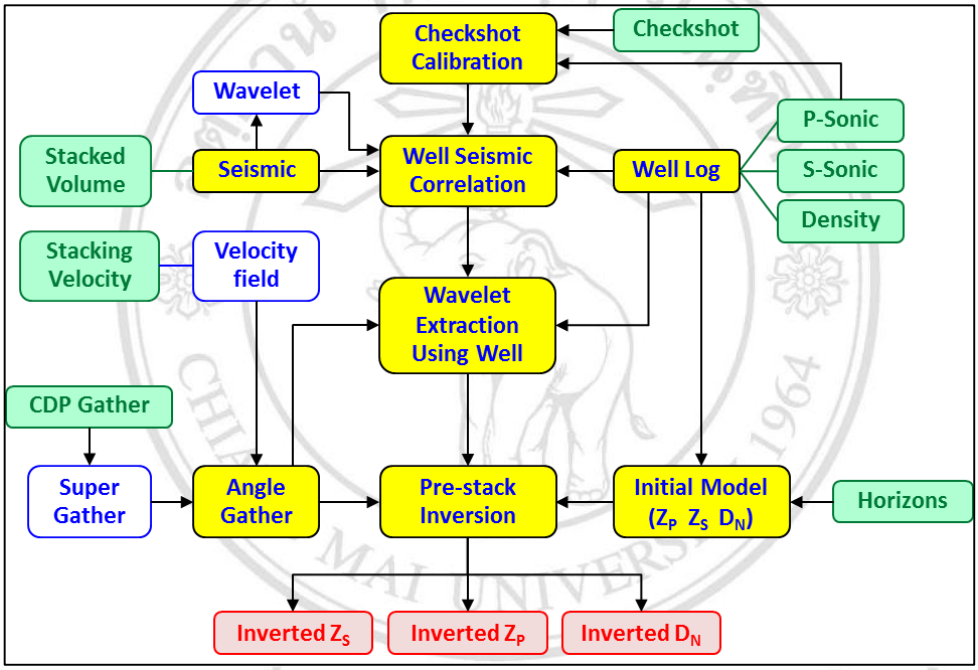

Figure 3-20. The workflow of pre-stack inversion (green boxes show input, red boxes show output, yellow boxes show processes, and white box show generated data)

Details of the workflow of pre-stack inversion are descripted in each step as:

1. Loading well data including sonic, shear sonic, density and checkshot data, both sonic logs can be converted to compressional and shear velocity logs (V_P and V_S).

2. Calibrating P-sonic logs with checkshot data for time-depth conversion, the checkshot calibration modifies either the depth-time curve associated with a sonic log or the sonic velocities to improve the tie between a synthetic and real seismic data.

3. Loading the post-stack seismic data (or stacked gathers) is necessary for extracting statistical wavelet from seismic data (Figure 3-21).

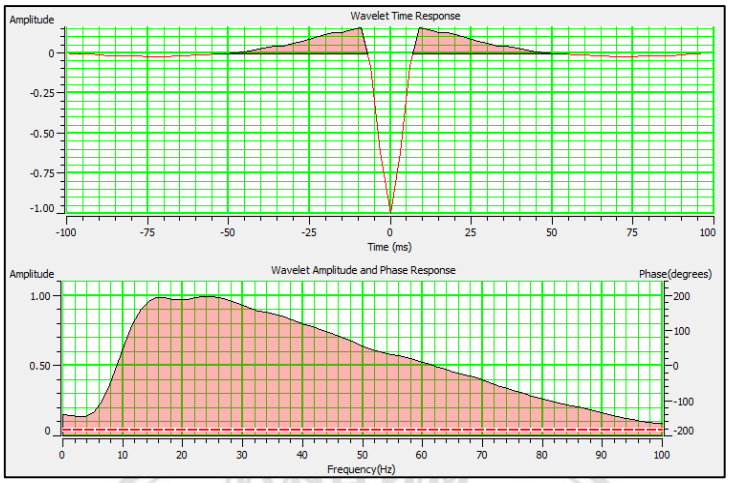

Figure 3-21. Statistical wavelet is extracted from full range of post-stack seismic and 180° phase rotation to match with data polarity using for seismic-well tie.

4. Correlating each well to the seismic volume optimizes the depth-time conversion and residual static correction. The correlation is calculatedly shifted a log to improve the time correlation between the target log and the seismic volume. Bulk shift is applied for matching the well log depth-to-time data to the measured seismic times.

5. Loading pre-stack seismic data (or CDP gathers) uses for pre-stack inversion, and conditioning the seismic data is muted bad signal. The mute option applies an offset-dependent mute (or ramp) to a range of pre-stack gathers. Muting is essential to remove stretched signal at far offsets, so only the reliable data is kept for the gather.

6. Converting CDP gathers to super gathers, this process analyses a subset of gathers, and calculates a number of "super-gathers", where each trace represents a range of offsets. Therefore, it forms average common depth points to enhance the signal-to-noise ratio by collecting adjacent them and adding them together (Figure 3-22).

7. Generating velocity field uses stacking velocity data for angle gather conversion. The velocity source can be selected from data volume of the existing seismic model, time-depth curve or sonic log curve of single well, strata model, and velocity table of control points with location-time-velocity (stacking velocity).

8. Converting super gathers to angle gathers, this process allows transforming a subset of gathers from the offset domain into the incident angle domain. This shows the distribution of incidence angels at the zone of interest which inputs decision parameters.

This step is necessary for pre-stack data which is intended for pre-stack inversion since the inversion only works on angle gathers (Figure 3-23).

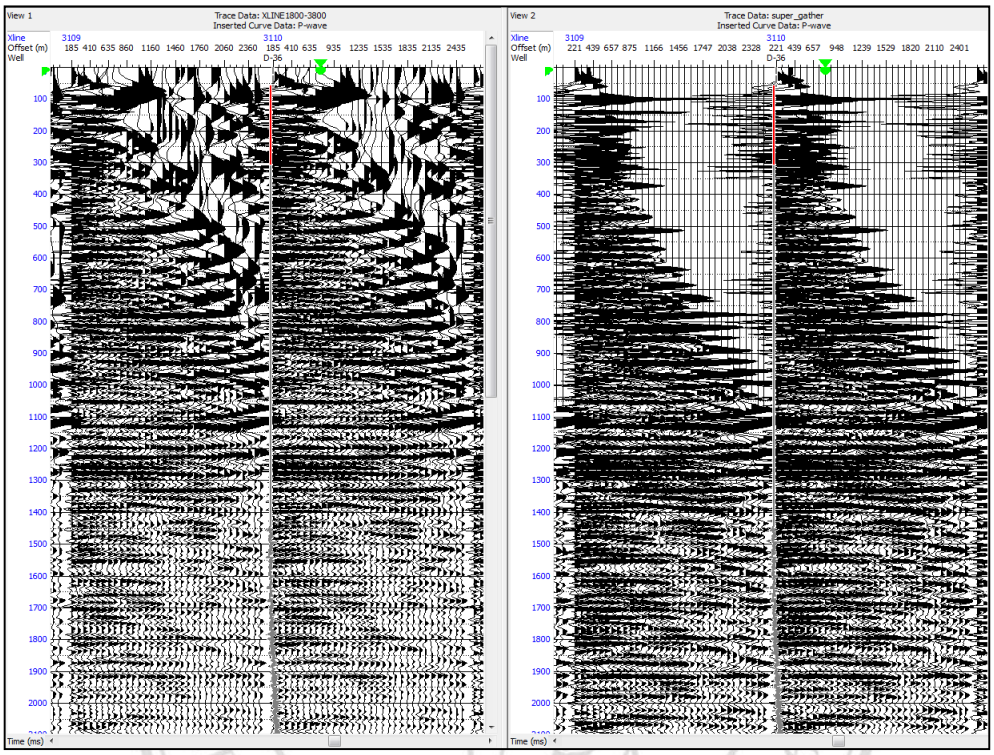

Figure 3-22. CDP gathers (left) and super gathers after muting (right)

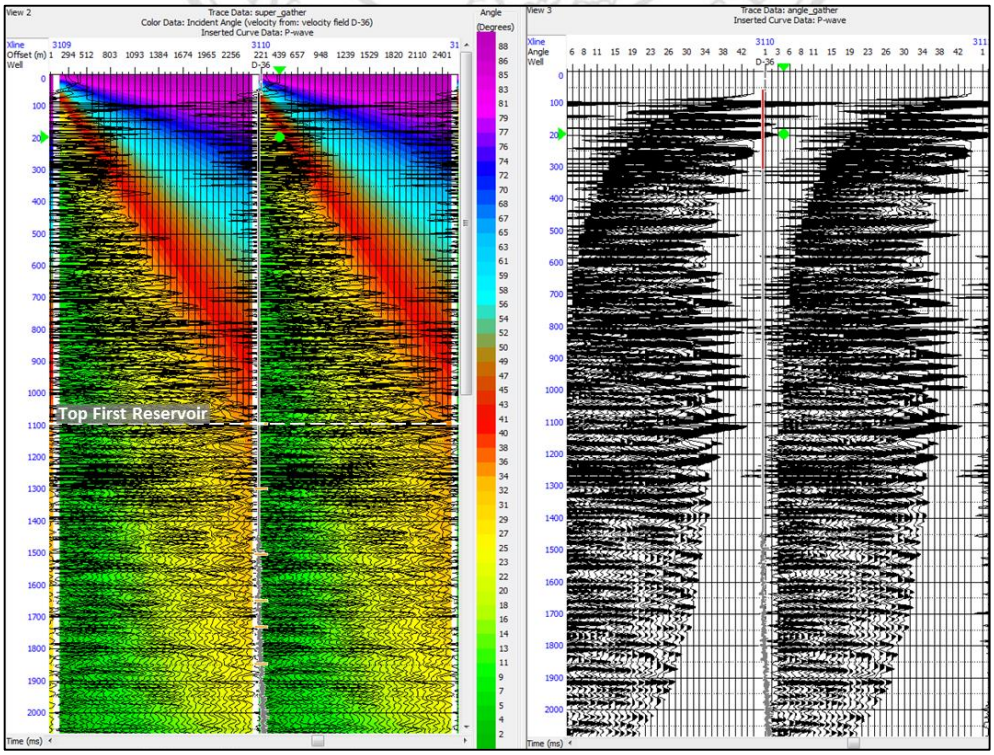

Figure 3-23. Super gathers overlying incidence angle (left) and angle gathers (right)

9. Loading horizons, the most horizons pick from post-stack seismic, so the values are drawn flat across each gather (Figure 3-24).

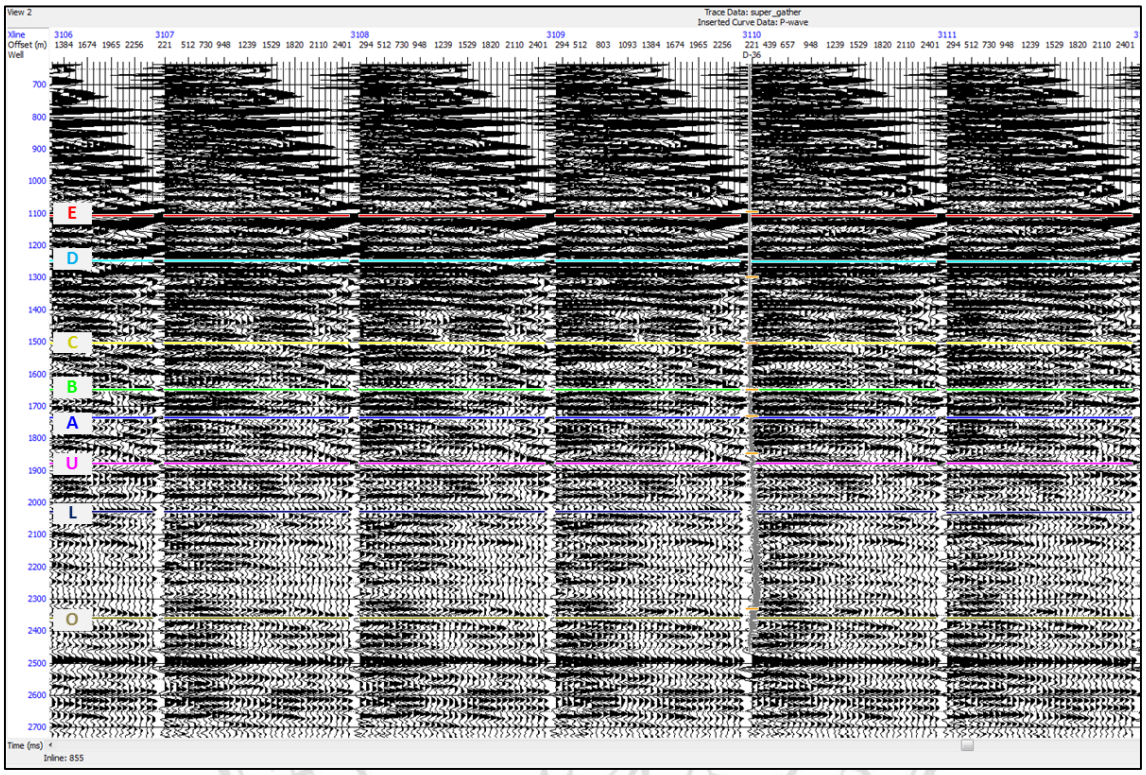

Figure 3-24. The picking horizons on pre-stack seismic data

10. Extracting a group of wavelet is performed after conducting seismic-well tie. The series of angle-specific wavelets work better in seismic-well correlation and cross-correlation between the wavelet and synthetic traces for pre-stack seismic inversion (Figures 3-25 and 3-26).

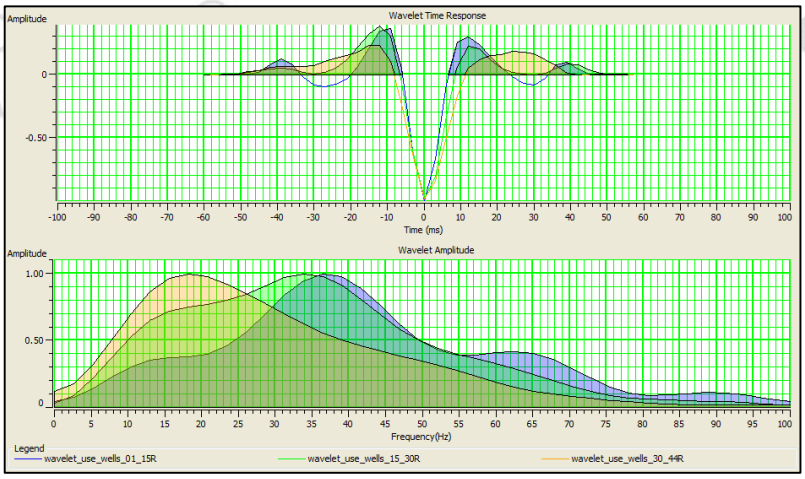

Figure 3-25. A series of wavelets extraction from well using for seismic inversion

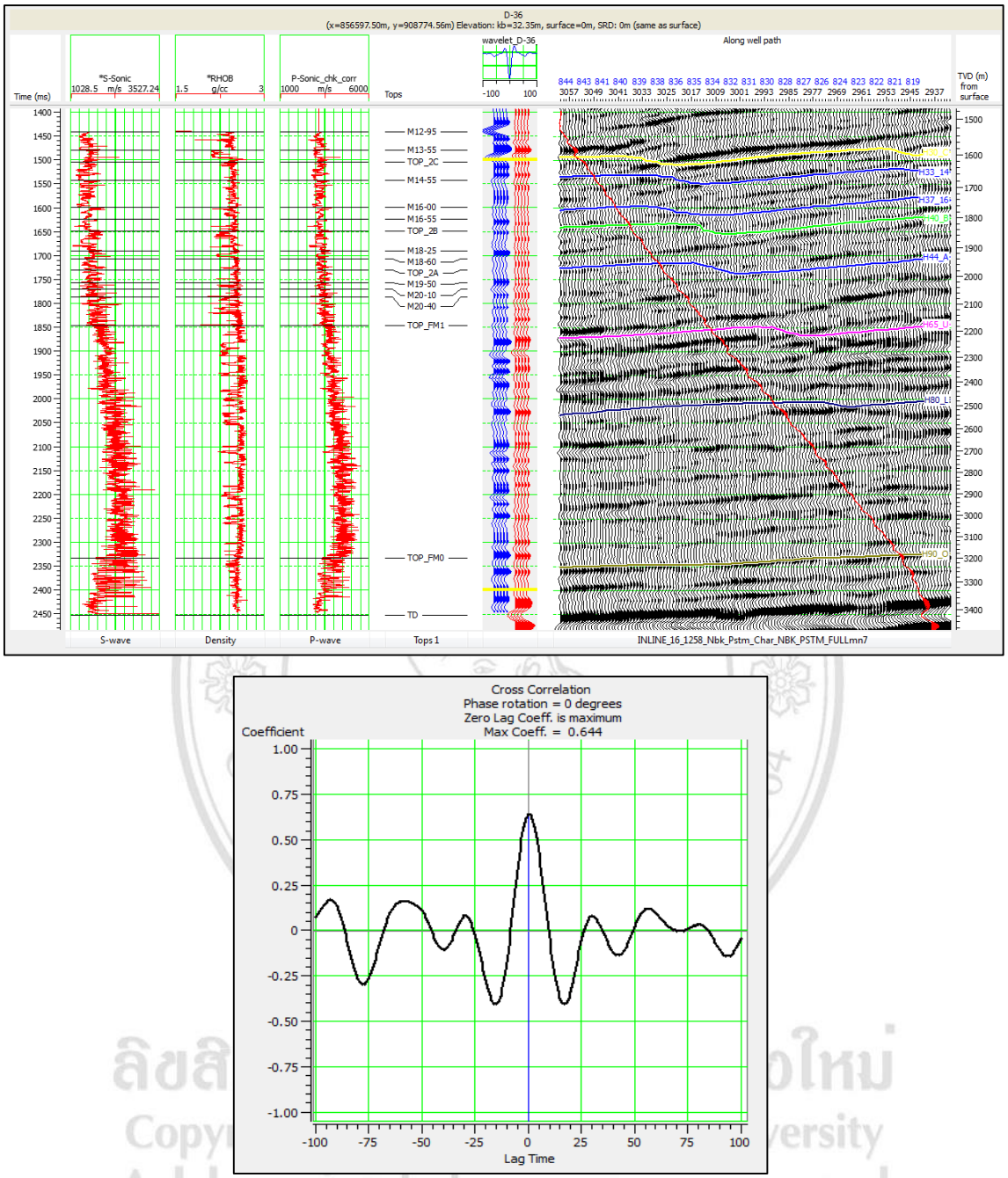

Figure 3-26. Seismic to well correlation and cross-correlation using single wavelet

11. Generating initial strata models of P-impedance, S-impedance and density using wells combines with stacking velocity and uses picking horizons as guide to interpolate physical property between wells. Strata models are volumes defining an interpreted seismic parameter such as velocity, reflectivity or impedance. They attempt to define the study area in geological properties more than seismic reflectors, so they are similar to a stratigraphic model (Figure 3-27).

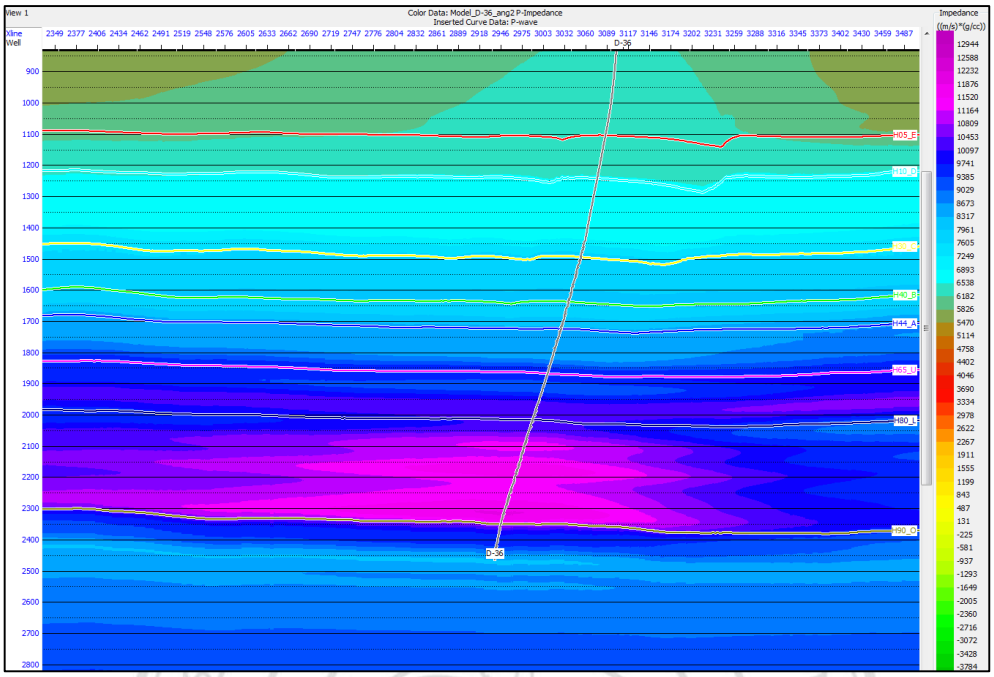

Figure 3-27. Cross section of P-impedance initial strata model

12. Running inversion analysis determines the best inversion parameters. The inversion analysis performs an inversion on selected well locations that means the inversion parameters can be quickly tested. This process creates inverted synthetics of velocity and density to compare to the actual curves at well locations (Figure 3-28). Then run the inversion model applying to seismic volume.

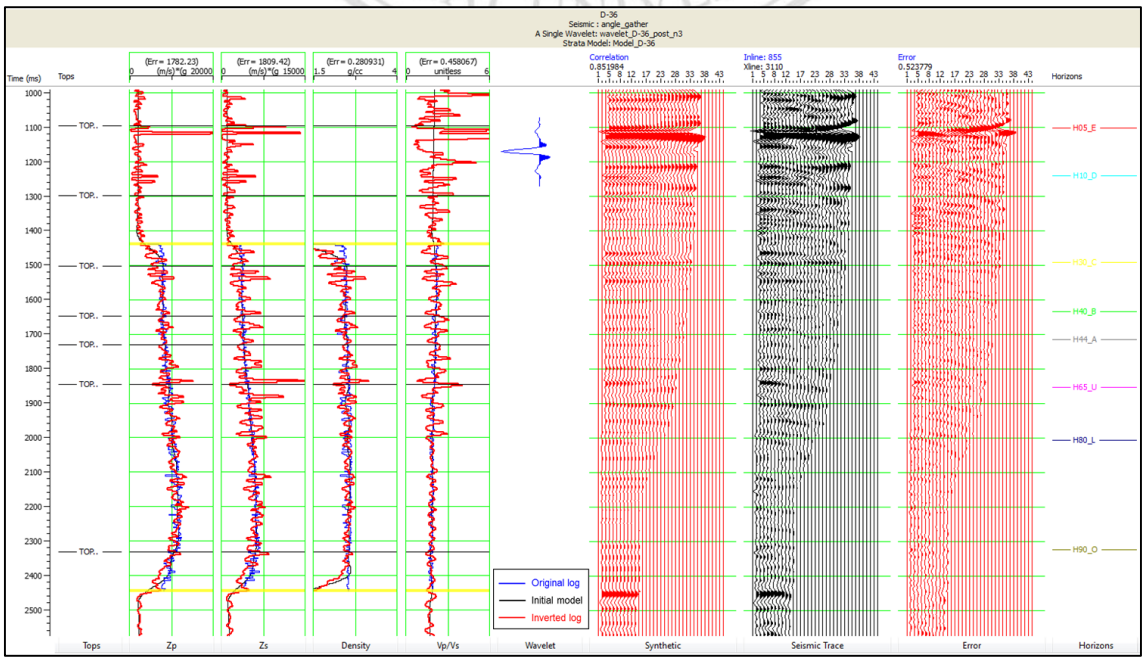

Figure 3-28. Example of pre-stack inversion analysis at D-36 well

13. Analysing the results is matched between each inverted volume and well log data at well location. The acceptable results should be saved and applied to volume, unless the inversion parameters should be changed and re-run again. Examples of inversion models are illustrated in Figure 3-29.

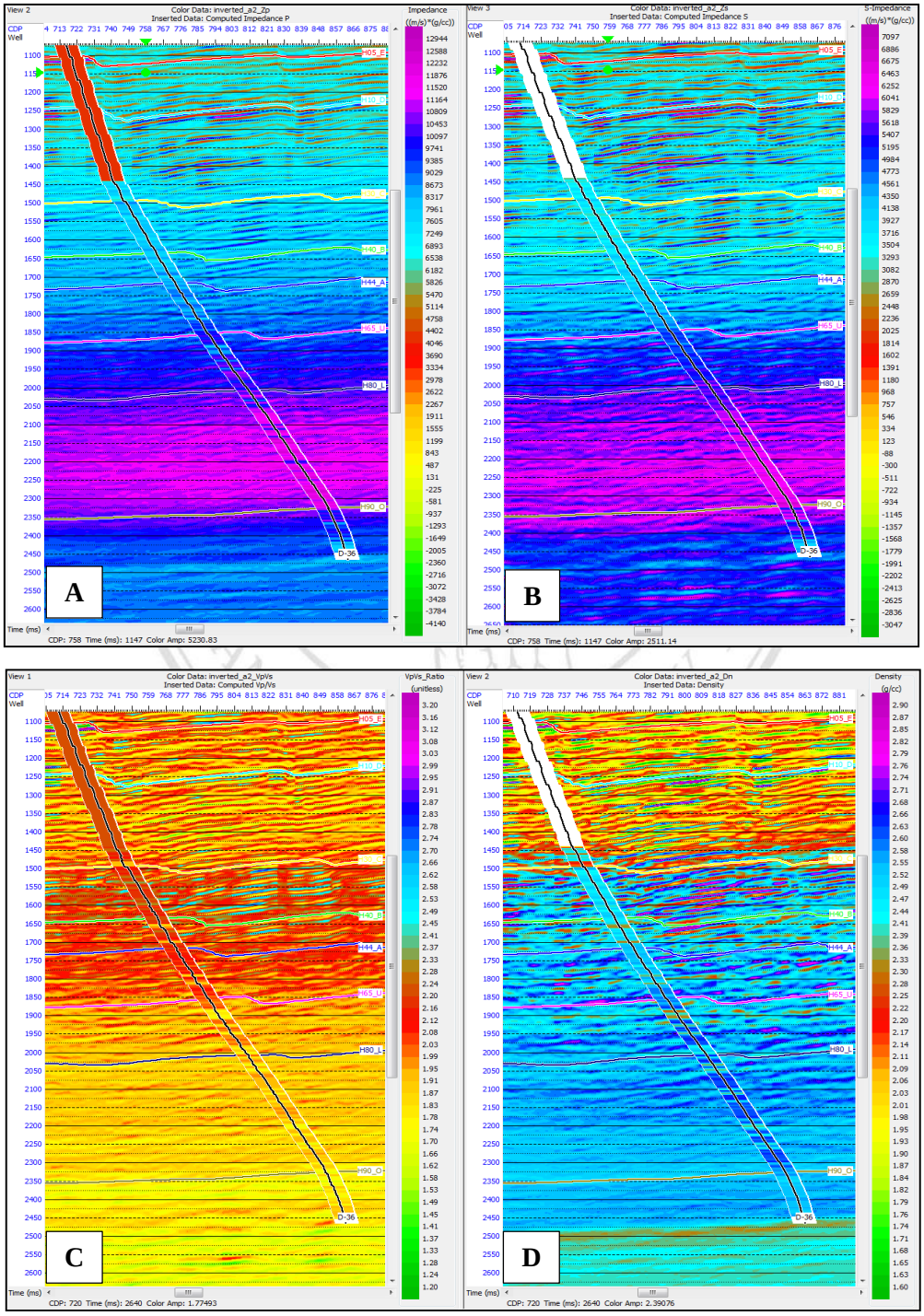

Figure 3-29. Example results of the pre-stack inversion models along D-36 well A) Inverted Z_P B) Inverted Z_S C) Inverted V_P/V_S and D) Inverted density

3.4 Lithology Delineation and Prospect Identification

The selection of inverted model sets derived from pre-stack seismic inversion for lithology delineation and prospect identification are analysed from lateral and vertical distribution of inversion results such as the inverted P-impedance, inverted S-impedance and inverted V_P/V_S model. In theoretically, to compare P-impedance and S-impedance values in same section and location at which hydrocarbon is located, the S-impedance should show relatively high impedance because the S-wave velocity is slightly increase within a hydrocarbon reservoir. In contrast to the P-wave, the P-wave velocity would be decreased dramatically within a reservoir (Gassmann, 1951). Therefore, the V_P/V_S would be expected to decrease significantly within the hydrocarbon reservoirs.

It is important to co-operate the seismic inversion, rock physics model and AVO response for lithology delineation. In reason, the data at well locations is acquired from true subsurface lithology, the delineation using well information should be done and then is used to typical pattern for area without well data.

For prospect identification, the prospects can be normally defined with other petroleum system analysis such as traps and seals, after the sandstone reservoirs were delineated by seismic inverted models.